

## Article

# Climate Drivers and Sources of Sediment and Organic Matter Fluxes in Intermittent Rivers and Ephemeral Streams (IRES) of a Subtropical Watershed, USA

Janet Dewey <sup>1,\*</sup>, Jeff Hatten <sup>2</sup> , Byoungkoo Choi <sup>3</sup>, Clay Mangum <sup>4</sup> and Ying Ouyang <sup>5</sup>

<sup>1</sup> Geology and Geophysics Dept. 3006, University of Wyoming, 1000 E. University Ave, Laramie, WY 82071, USA

<sup>2</sup> Forest Engineering, Resources & Management, Oregon State University, 280 Peavy Hall, Corvallis, OR 97333, USA; Jeff.Hatten@oregonstate.edu

<sup>3</sup> Department of Forest Environment Protection, Kangwon National University, Chuncheon 200-701, Korea; bkchoi@kangwon.ac.kr

<sup>4</sup> Weyerhaeuser NR Company, 406 Cole Rd., Hattiesburg, MS 39402, USA; clay.mangum2@weyerhaeuser.com

<sup>5</sup> USDA Forest Service, 775 Stone Blvd., Thompson Hall, MS 39762, USA; ying.ouyang@usda.gov

\* Correspondence: jdewey2@uwyo.edu; Tel.: +1-307-223-2265

Received: 28 August 2020; Accepted: 10 October 2020; Published: 16 October 2020



**Abstract:** Climate-driven hydrological models rarely incorporate intermittent rivers and ephemeral streams (IRES) due to monitoring difficulties and their perceived minor effect on river networks. Worldwide, IRES represent approximately 50% of river networks and up to 60% of annual flow and are recognized as conduits and processors of organic matter (OM). Climate induced changes in precipitation and discharge (Q) may impact OM fluxes from IRES. We assessed storm-driven source and flux of total suspended solids (TSS) and OM from small IRES in Mississippi, USA. We used linear Pearson correlations to evaluate relationships between water and storm characteristics (e.g., discharge). Stepwise regression was used to predict change in flux. Dissolved OM was derived from saturated flow through soil whereas particulate OM was derived from channel extension during storms. A power log relationship between Q and materials flux indicated that Q was the driver for flux. A 5% increase in Q within IRES may result in flux increase of 2% TSS and 1.7–2.8% OM. Climate change projections of increased storm intensity over a shorter water year will increase channel extension and soil water transfer resulting in higher material flux to downstream reaches. Climate-driven hydrological models of OM flux should incorporate IRES.

**Keywords:** climate change; IRES; OM; DOC; POC; ephemeral stream; event sampling; headwaters

## 1. Introduction

Intermittent rivers and ephemeral streams (IRES) have long been perceived as peripheral in their effect on river networks because they only flow in response to rainfall [1,2]. It has been estimated that headwater IRES account for 60% of total mean annual flow (for streams and rivers in the northeastern US) [3] and approximately 50% of the world's total river networks [4]. Intermittent rivers and ephemeral streams drain and connect with much of the Earth's critical zone, so they have considerable potential to release, transport, transform, or sequester organic matter (OM) (e.g., [5,6]); this, in turn, can be released into the atmosphere in the form of CO<sub>2</sub> [7,8]. Approximately 36% of the CO<sub>2</sub> outgassed by river networks can be attributed into headwater streams [8]. Climate change can affect the timing, duration, frequency, and severity of storm events—all of which have the potential to control sediment and OM exports from IRES [9].

Organic matter is a transport vehicle for nutrients, carbon, and pollutants, all of which regulate or impact biological processes [10,11]. Production, transport, degradation, preservation, and sorption of OM are influenced by complex biological, chemical, and hydrological interactions [11–13]. Increases in temperature, precipitation, discharge, and groundwater connectivity associated with climate change may accelerate chemical and physical processes governing OM dynamics [14–19]. Therefore, understanding the source–transport–transform–sink behavior of OM in ephemeral streams (ES) is critical to predicting how OM will affect downstream processes and water quality.

Ephemeral streams function as collection sites for organic inputs and typically flow in response to storm events as infiltration excess [20] or saturated excess [21] overland flow with little or no connectivity to the water table (e.g., Table 1 in Reference [22]). Episodic connectivity during precipitation and flow pulses permits transport of OM, including dissolved and particulate C, to downstream perennial reaches. Storms are important drivers for material flux in headwaters; approximately 90% of dissolved and particulate material in headwater streams is exported during storm events [23]. This flux occurs disproportionately during high flow and is often a power function of the discharge rate [24–26]. Ephemeral streams have been poorly studied in comparison to their intermittent and perennial counterparts with regard to nutrient and energy fluxes due to the fact of their measurement difficulties and rapid discharge (i.e., “flashy behavior”).

Recent research suggests that in-channel processing of OC within small inland watersheds is a regionally important source of atmospheric CO<sub>2</sub> [7,8,27]. Frequent wetting and drying cycles that occur in ephemeral streams provide “hot moments” [28] for dissolved organic matter (DOM) production, transformation, and transport. A number of studies have shown that oscillation between wet and dry stream conditions facilitates dissolved organic carbon (DOC) processing (e.g., [29–31]) and CO<sub>2</sub> evasion [32]; therefore, even very small ephemeral streams may be key components of C cycling in riverine systems [33].

Current climate change scenarios predict an increase in the frequency of droughts and high magnitude storm events in the southeastern United States even if mean annual precipitation (MAP) does not change [34]. Predicted changes in frequency [35] and severity of precipitation [36] may increase effective sediment and OC transport processes [37–39]. Equally, the dry component of the wet–dry cycle of ephemeral streams will increase both spatially and temporally as temperatures rise [32] thereby increasing DOM production [40]. Much of the research on streams that exhibit wet–dry cycles has focused on arid and semi-arid regions [41] and neglected ephemeral streams in humid climates. Therefore, understanding the behavior of C in temporary streams of humid ephemeral source areas is important for understanding the contributions of those source areas to C dynamics in general and under accelerated transport efficiency as predicted by some climate change scenarios. Our research was guided by two questions: (1) what are the sources of sediment and OM in IRES and (2) what are the controls on the flux of sediment and OM from very small (<4 ha) IRES to downstream reaches? We used chemical characteristics to determine the source and behavior of OM during storm events within small ephemeral catchments and tracked the behavior of potential exports during storm events. We discuss the implications of our study in the context of climate change.

## 2. Materials and Methods

### 2.1. Study Design

We studied a 32 ha watershed (33°30′49.00″ N, 89°25′40.00″ W) within the Upper Gulf Coastal Plain in Webster County, Mississippi. The site has a humid subtropical climate with a mean temperature ranging from 7 °C in winter to 26 °C in summer (US National Weather Service Station #222896, Eupora, MS, USA). The 30 year mean annual precipitation is 1451 mm, much of which falls during winter and spring. Annual discharge is  $240 \times 10^3 \text{ m}^3 \text{ year}^{-1}$  [42]. Soils are well- to moderately well-drained Sweetman series: US Department of Agriculture (USDA) taxonomy = fine, mixed, semiactive, thermic Typic Hapludult; World Reference Base (WRB) taxonomy = Profondic Alisol. Soils are high in clay

with A-horizons of either loam or silt loam; pH ranges from 4.5 to 5.5. Slopes are steep, soils are erodible, and dominant land use is woodland [43]. Forest vegetation is characteristic of the southeastern Mixed Forest Province and consists of even-aged loblolly pine (*Pinus taeda* Linnaeus) with a smaller component of mixed hardwoods; a detailed description is provided in Reference [44]. The site has been in pine timber production for 30 years.

Four small ephemeral catchments, nested within a perennial stream watershed (Figure 1), were monitored for dissolved and particulate contributions to downstream water. We used the following field criteria [22] to classify streams: (1) weakly defined channels; (2) interrupted flow, most of which was in response to storms; (3) a water table below the channel surface for most of the year; (4) lacking in aquatic insects; (5) lacking in obvious material transport; (6) scoured beds; and (7) intermittent organic buildup. Ephemeral streams were mapped as depressions by the US Geological survey (1983). We classified the streams as ephemeral based on the aforementioned criteria, recognizing that the boundary between ephemeral and intermittent classification is approximate. Our major focus in this study was on the ephemeral streams (ES) of the IRES.

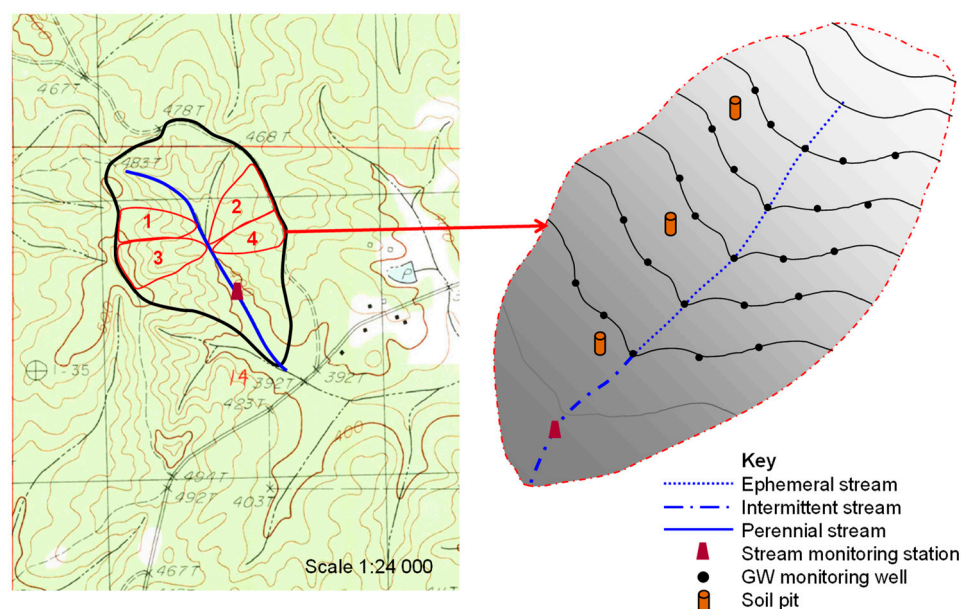


**Figure 1.** Schematic project layout depicting monitored ephemeral catchments in the study watershed. Numbers 1–4 correspond to the named ephemeral 1–4 watersheds described in this study. Topographic base excerpt are from the Little Sand Creek, Mississippi quadrangle [45].

For monitoring purposes, we defined the upstream limits of the ES segments by the upslope limit of channel development; downstream limits were defined by evidence of a clearly defined channel, over bank deposits, and seasonal streamflow [44]. All monitored ES lacked evidence of a persistent intermittent segment: the ES conducted surface water directly to the perennial stream and flowed in response to storm events. However, storm events in this region occurred frequently enough that steady-state flow (hereafter referred to as base flow) was periodically observed at the downslope limits of the channels. The ES watershed size ranged from 1.8 to 3.8 ha; the remainder (20.6 ha) comprised a mix of uncut and recently cut forest (Table 1) which had recovered for two years prior to monitoring for this study. Soil disturbance and forest cover were not a focus of this paper but are described as a frame of reference for interpreting OM dynamics in the watersheds. Ephemeral channels differed in their forest cover (Table 1 and described in References [44,46]) and were chosen to represent a continuum of soil disturbance and forest cover that may influence OM dynamics.

**Table 1.** Watershed characteristics and sampling record.

Watershed	Watershed Size (ha)	Stream Length (m)	Harvest Treatment	Length of Q Record (months)	Total Q ( $\times 10^3 \text{ m}^3 \text{ year}^{-1}$ )	Storm Flow Samples	Base Flow Samples
Ephemeral 1	2.4	78	* Reference	14.9	27.13	67	14
Ephemeral 2	3.6	83	<sup>†</sup> BMP2	14.8	5.49	82	21
Ephemeral 3	3.8	92	<sup>‡</sup> BMP1	14.0	27.79	14	6
Ephemeral 4	1.8	81	<sup>§</sup> CC	15.3	4.99	40	10
Ungaged Ephemeral	20.6	-	-	-	-	-	-
Ephemeral Average					173.51		
Perennial	32.2	-	-		239.91	30	30

Total Q was calculated from all Q measurements across the entire length of the record. \* Reference site at which no harvesting has occurred since 1978. <sup>†</sup> Riparian buffer in which logging debris was not permitted in the ephemeral drainage channel. <sup>‡</sup> Riparian buffer in which logging debris was permitted in the ephemeral drainage channel. <sup>§</sup> Clearcut with all merchantable timber removed and no riparian buffer.

## 2.2. Field Sampling

Ephemeral streams (Figure 2) were equipped with stations to monitor stream flow and collect event samples over 17 months (17 February 2010 to 13 July 2011). A 1.8 m long, 254 mm diameter PVC pipe was installed at the outlet of each ephemeral watershed to constrain flow within a measurable cross-sectional area. Water depth, velocity, and discharge within pipes were measured by area velocity sensors controlled by flow loggers (ISCO Inc., Lincoln, NE, USA) programmed to record at 15 min intervals. Discrete water samplers (ISCO Inc., Lincoln, NE, USA) were linked to flow loggers and programmed to start collecting samples on the rising limb of each event. Event sampling was triggered by a 20 mm increase in flow depth in the pipe over a 15 min interval. Discrete samplers were programmed to cease sampling as velocity and/or depth reverted to pre-event levels. Flow was variable among streams and events, so the number and timing of sampled storm events differed among streams. Steady-state base-flow samples were hand-collected from pipe outflow when possible.



**Figure 2.** Left: Gauged reference stream with a 254 mm diameter pipe, ISCO sampler, and flowmeter. Right: Ephemeral stream flowing during storm event.

The perennial stream monitoring station was located 200–300 m downstream from ephemeral monitoring stations. Perennial stream stage was measured with a pressure transducer (In-Situ Level TROLL 300) inside a stilling well (91.8 cm tall, 152 mm diameter). Velocity was measured using a portable flowmeter (Hach Company, Loveland, CO, USA). Discharge was determined using a stage-discharge rating curve, developed from 15 measurements of stream profile, stage, and velocity measurements across a range of flows. The perennial stream was equipped with an area velocity sensor and a discrete sampler which was programmed to initiate sampling in the event of increased



depth and/or flow. Base-flow samples were hand-collected during field visits when discharge was at steady state.

Groundwater, precipitation, canopy throughfall, and soil pore-water samples were used to characterize potential source contributions to streamflow. Groundwater was sampled in ephemeral watersheds via a grid of wells arranged in five transects perpendicular to the stream channel; each transect contained five wells spaced at 5 m intervals. Wells were made of 5 cm inner diameter PVC pipe and screened the entire subsurface interval. Wells penetrated to a depth of 2.5 m or until refusal. Well water was sampled monthly using a bailer with a check ball after purging wells. Depth of sampling for the groundwater source varied depending upon well and time period [44,46]. Regional precipitation data (15 min interval) for the period 10 February 2010 to 30 May 2010 were acquired from the Eupora 2E, MS, US (33.56° N, 89.24° W) National Oceanographic and Atmospheric Administration (NOAA) weather station [47]. Onsite precipitation data were collected for the period 30 May 2010 through 13 July 2011 using a tipping bucket rain gauge (ISCO Inc., Lincoln, NE, USA) installed in an open area of the watershed. Precipitation and canopy throughfall were sampled using acid-washed plastic 18.9 L buckets with nylon window screens over the top to prevent contamination by fallen debris. Zero-tension lysimeters collected soil pore water four times during the spring of 2011 at three depths within the soil profile (O, A–10 cm, and A–20 cm). O, A, B, and C soil horizons were sampled from soil pits at representative locations (Figure 1).

### 2.3. Sample Analysis

We examined the source and flux of water and OM. The flux of OM from IRES is partially controlled by the concentration of the material in the water, which is strongly controlled by source. To understand how climate change will affect the flux of the materials, we must understand the source and mobilization processes of OM.

Water samples were fractionated in the lab into dissolved and particulate components. Samples were filtered to collect particulate matter (PM) through 0.7 µm glass fiber filters (GFFs) that were pre-combusted for 4 h at 350 °C to remove organics. The PM-laden filters were oven-dried overnight at 60 °C and weighed for total suspended solid (TSS) concentration. Filtrate was collected and frozen for analysis of dissolved constituents. Soils and suspended sediment were analyzed for total C and N. Soils were dried overnight at 70 °C, ground to pass a 60 mesh sieve, and dried again prior to analysis. Dried, sediment-laden GFFs were subsampled using a single-hole-punch tool. Samples were analyzed for total organic carbon (OC) and N by flash combustion elemental analyzer (Costech ECS 4010, Valencia, CA, USA). Molar ratios are used where N:C data are presented. Particulate organic carbon (POC) concentration ( $\text{mg L}^{-1}$ ) was calculated as:  $\text{POC (mg L}^{-1}\text{)} = \text{g of carbon (from NC analysis)} / (\text{area of filter subsampled (cm}^2\text{)} / \text{area of whole filter (cm}^2\text{)})$ . The OC concentration of sediment was calculated as:  $\% \text{OC} = \text{POC (mg L}^{-1}\text{)} / \text{TSS (mg L}^{-1}\text{)} * 100$ .

Filtrate was analyzed for chloride ( $\text{Cl}^-$ ), nitrite ( $\text{NO}_2^-$ ), nitrate ( $\text{NO}_3^-$ ), and ammonium ( $\text{NH}_4^+$ ) by ion chromatography (Dionex DX–500, Sunnyvale, CA, USA). We measured ultraviolet absorbance at 254 nm ( $\text{UVA}_{254}$ ) using a BioMate3 spectrophotometer with a 1 cm cell in order to have a low-cost measurement to correlate with DOC and be able to convert dissolved organic carbon to specific UV absorbance ( $\text{SUVA}_{254}$ ) which provides insight into the nature of the organic matter present (e.g., high  $\text{SUVA}_{254}$  indicates dominance of humic matter and, thus, a soil origin for DOC). Total nitrogen (as TKN) was converted to ammonium cation by sulfuric acid digestion with mercuric oxide catalysis in a microwave digester (MARS X Press, CEM, Matthews, NC, USA). Samples were digested for one hour with a 15 min ramp time and 45 min hold time at 200 °C and analyzed for TKN by salicylate method on a Technicon Autoanalyzer III wet chemistry analyzer (Bran + Luebbe, Norderstedt, Germany). Dissolved inorganic nitrogen (DIN) was determined as sum of nitrite-N ( $\text{NO}_2\text{-N}$ ), nitrate-N ( $\text{NO}_3\text{-N}$ ), and ammonium-N ( $\text{NH}_4\text{-N}$ ). Dissolved organic nitrogen (DON) was calculated as total N minus DIN. We used DON:DOC and PON:POC (rather than the more commonly used DOC:DON and POC:PON) herein because it is statistically more robust due to the higher number (%OC) in the denominator.

Filtered, frozen water, suspended sediment, and soils were sent to the UC Davis Stable Isotope Facility and analyzed within 2 months of sample collection. Dried soils needed no preservation; water samples were preserved by filtering with a 0.2 micron filter and frozen according to UC Davis standard operating procedures. Water was analyzed for DOC and DOC  $\delta^{13}\text{C}$  PDB using an OI Analytical model 1030 TOC Analyzer (OI analytical, College Station, TX) interfaced to a PDZ Europa 20–20 Isotope Ratio Mass Spectrometer (Sercon Ltd., Cheshire, UK) with a GD–100 gas trap interface (Graden Instruments). Stable isotopic composition of particulate organic carbon (POC;  $\delta^{13}\text{C}$ ) and particulate organic nitrogen (PON;  $\delta^{15}\text{N}$ ) were determined by flash-combustion elemental analysis coupled with isotope-ratio mass spectrometry (EA-IRMS; Elementar Analysensysteme GmbH, Hanau, Germany) interfaced to a PDZ Europa 20–20 isotope ratio mass spectrometer (Sercon Ltd., Cheshire, UK). Isotopic data for C and N were reported in standard delta notation (‰ per mil) relative to Pee Dee Belemnite (PDB) and air standards, respectively. Standard reference materials covering a range of  $^{13}\text{C}$  and  $^{15}\text{N}$  signatures were used to evaluate precision and accuracy of mass spectrometer response; analytical precision for  $\delta^{13}\text{C}$  of DOC was 0.4‰; precision for  $\delta^{13}\text{C}$  and  $\delta^{15}\text{N}$  was tighter than 0.3‰.

#### 2.4. Data Analysis

Average concentrations of measured stream water constituents were calculated for each gauged watershed for the length of the study. To determine the effect of storm-specific attributes on composition of dissolved and particulate material, individual flow events were delineated by the change in discharge. The beginning of an event within ES was defined as (1) any discharge  $>0.002\text{ m}^3\text{ s}^{-1}$  or (2) rate of change in discharge  $>0.0002\text{ m}^3\text{ s}^{-1}\text{ 15 min}^{-1}$  or (3) start of flow. The beginning of an event within perennial streams was defined as any discharge  $>0.002\text{ m}^3\text{ s}^{-1}$ . Where there was a one-hour decline in discharge, followed by an increase in discharge, the event clock was reset, and a new event began. Linear Pearson correlations of log-transformed data were used to evaluate relationships between independent event variables and dependent surface water concentrations and characteristics. We chose event variables that were likely to affect the flux of sediment and OM within our watersheds. Independent event variables tested included: rate change in Q over time; water year date (number of days after 1 October (which was the beginning of the water year); time since flow began in hours; time since event initiation; and time before or after peak flow. Event variables are defined as: Precipitation = the amount of precipitation that fell in the previous 15 min; Q = instantaneous discharge at the time the sample was collected; PeakTime = time before or after peak flow; FlowTime = time since flow began in hours; RateChange = change in Q over time where positive values are on the rising limb and negative values are on the receding limb; EventTime = time since event initiation; WY Day = number of days after 1 October (beginning of water year). Stepwise multiple linear regression was used to explore relationships among event variables and surface water characteristics; data were log-transformed to meet assumptions of normality. The lm function in base R [48] was used to model constituent fluxes from independent event variables; step Akaike Information Criteria (stepAIC function) from the MASS package [49] was used to optimize the size of the model. Herein, we report the standardized coefficients with adjusted  $R^2$  and whole-model  $p$ -values for purposes of examining the relationships among variables as well as the coefficients and equation used to develop predictive calculations. All estimates of mass fluxes were calculated using instantaneous flow-weighted averages across all storms and streams of within-event measurements.

### 3. Results and Discussion

#### 3.1. Physical and Chemical Attributes

Over the 17 month study period, 16 events generated discharge in one or more streams (Table 2). Precipitation was monitored for 12 months (May 2010 through May 2011; Figure 2) and ranged from 21–110 mm per event with a mean of 55 mm. The maximum precipitation rate occurred at the onset of an event and ranged from 10–72  $\text{mm h}^{-1}$  with a mean of 36  $\text{mm h}^{-1}$ . Precipitation between January

and May accounted for 53% of the annual total and 94% of the discharge events over 15 months. Event duration ranged from 1.0 h to 22.3 h with a mean of 8.0 h. Precipitation events triggered 233 flow event samples ranging from a total of 14 to 82 samples per watershed per event (Table 1). Mean event discharge across all recorded events for ephemeral and perennial streams was 749 m<sup>3</sup> event<sup>-1</sup> and 7324 m<sup>3</sup> event<sup>-1</sup>, respectively.

**Table 2.** (A) Average instantaneous flow-weighted within-event values of selected dissolved and particulate stream water constituents across all sampling times. (B) Average values from potential sources.

(A)	Ephemeral 1	Ephemeral 2	Ephemeral 3	Ephemeral 4	Ephemeral Average	Perennial	Pr > Chi-Square
TSS (mg L <sup>-1</sup> )	342.6 ± 74.4	1713.0 ± 708.1	54.1 ± 14.8	154.7 ± 31.3	566.1 ± 386.9	101.1 ± 46.3	<0.0001
POC (mg L <sup>-1</sup> )	21.3 ± 11.0	8.06 ± 1.31	2.27 ± 0.43	5.54 ± 1.79	9.30 ± 4.18	3.46 ± 0.96	0.0004
DOC (mg L <sup>-1</sup> )	11.6 ± 1.9	13.54 ± 0.97	15.15 ± 0.97	17.73 ± 1.42	14.51 ± 1.29	5.83 ± 1.07	<0.0001
Cl (mg L <sup>-1</sup> )	1.89 ± 0.10	1.65 ± 0.07	1.69 ± 0.22	1.26 ± 0.11	1.62 ± 0.13	2.91 ± 0.14	<0.0001
UVA <sub>254</sub> (cm <sup>-1</sup> )	0.55 ± 0.03	0.47 ± 0.02	0.44 ± 0.05	0.76 ± 0.03	0.56 ± 0.07	0.19 ± 0.02	<0.0001
SUVA <sub>254</sub> (L mg <sup>-1</sup> M <sup>-1</sup> )	4.1 ± 0.4	3.56 ± 0.13	3.51 ± 0.18	4.05 ± 0.17	3.79 ± 0.15	4.04 ± 0.49	0.992
DON:DOC	0.17 ± 0.06	0.11 ± 0.03	0.10 ± 0.02	0.04 ± 0.01	0.11 ± 0.03	0.30 ± 0.08	0.0003
DOC-δ <sup>13</sup> C	-27.20 ± 2.15	-28.50 ± 0.09	-28.90 ± 0.12	-28.80 ± 0.16	-28.30 ± 0.39	-28.60 ± 0.16	0.4865
%OC	4.6 ± 0.5	2.9 ± 0.2	3.8 ± 0.4	4.9 ± 0.7	4.0 ± 0.5	5.3 ± 0.5	0.0012
POC:DOC	1.69 ± 1.24	0.88 ± 0.45	0.15 ± 0.02	0.26 ± 0.09	0.75 ± 0.35	0.67 ± 0.23	0.0470
PON:POC	0.08 ± 0.00	0.08 ± 0.00	0.10 ± 0.01	0.09 ± 0.00	0.09 ± 0.01	0.08 ± 0.00	0.6116
POC-δ <sup>13</sup> C	-25.10 ± 2.63	-27.47 ± 0.29	-27.58 ± 0.32	-27.31 ± 0.31	-26.86 ± 0.59	-27.66 ± 0.21	0.3550
PON-δ <sup>15</sup> N	0.91 ± 0.46	0.70 ± 0.25	2.05 ± 0.4	1.83 ± 0.69	1.37 ± 0.33	1.00 ± 0.63	0.7762
(B)	Precipitation	Throughfall	O-horizon	Mineral Soil	Ground Water		
DOC (mg L <sup>-1</sup> )	3.48 ± 1.56	21.82 ± 6.34	26.73 ± 3.43	11.6 ± 1.96	2.8 ± 0.32		
Cl (mg L <sup>-1</sup> )	0.82 ± 0.07	2.05 ± 0.28	1.91 ± 0.57	2.23 ± 0.4	3.52 ± 0.21		
UVA <sub>254</sub> (cm <sup>-1</sup> )	0.04 ± 0.02	0.44 ± 0.07	1.3 ± 0.04	0.5 ± 0.4	0.13 ± 0.02		
SUVA <sub>254</sub> (L mg <sup>-1</sup> M <sup>-1</sup> )	1.39 ± 0.34	2.94 ± 0.30	5.09 ± 0.64	4.78 ± 0.51	8.21 ± 2.25		
DON:DOC	0.36 ± 0.05	0.07 ± 0.01	0.16 ± 0.03	0.04 ± 0.00	0.28 ± 0.03		
DOC-δ <sup>13</sup> C	-26.60 ± 0.35	-29.40 ± 0.30	-30.3 ± 0.03	-28.7 ± 0.53	-28.2 ± 0.18		

Values are the mean ± standard error. Stream water values are the means of the base flow and event flow. The O-horizon and mineral soil values are from lysimeter solutions. %OC is the % of OC in sediment by mass. The *p*-values are from Mann–Whitney *U* tests between perennial and ephemeral streams.

Particulate constituent concentrations among ES were highly variable (Table 2-A). The TSS concentration ranged from 54.1 mg L<sup>-1</sup> to 1713.0 mg L<sup>-1</sup>, and POC concentrations ranged from 2.27 mg L<sup>-1</sup> to 21.33 mg L<sup>-1</sup>. Average ES TSS (566.1 mg L<sup>-1</sup>; instantaneous flow-weighted average across all streams and storms of within-event measurements; from Table 2) was higher than that of the perennial stream (101.1 mg L<sup>-1</sup>) by a factor of 5.6; thus, it appears that the perennial stream was a sink for suspended solids. Average ES POC concentration (9.30 mg L<sup>-1</sup>) was higher than that of the perennial stream (3.46 mg L<sup>-1</sup>) by a factor of 2.7.

Dissolved constituent values DOC, Cl, UVA<sub>254</sub>, and specific UV absorbance at 254 nm (SUVA<sub>254</sub>) were consistent among ES (Table 2-A). The UVA<sub>254</sub> of ES was consistently higher than that of the perennial stream, probably due to the average DOC being (14.51 mg L<sup>-1</sup>) 2.5 times higher than that of the perennial stream (5.83 mg L<sup>-1</sup>). The SUVA<sub>254</sub>, on the other hand, was similar among perennial and ES. The ES Cl concentration was consistently lower than that of the perennial stream indicating that the perennial stream acquired Cl from another source(s).

We quantified concentrations of five potential source contributors to surface waters: precipitation, canopy throughfall, O-horizon soil leachate, mineral soil leachate, and groundwater (Table 2). The DOC concentration increased from precipitation through the canopy as throughfall and O-horizon leachate then declined through the soil profile reaching a minimum in the groundwater samples suggesting that it was removed or diluted with depth. The Cl concentrations generally increased from the canopy through the soil and into the groundwater. The Cl concentration of ephemeral event water was similar to that of canopy throughfall and O-horizon soil, whereas the Cl concentration in perennial event water was most similar to that of mineral soil leachate and groundwater. There was a strong linear correlation

(Pearson's  $R = 0.923$ ,  $p < 0.001$ ) between  $\text{UVA}_{254}$  absorbance and DOC concentration, explaining the similar pattern between  $\text{UVA}_{254}$  and DOC. The  $\text{UVA}_{254}$  in precipitation was low but increased as water passed through the forest canopy. Highest  $\text{UVA}_{254}$  levels were observed in O-horizon leachates;  $\text{UVA}_{254}$  decreased with depth as water passed through the soil profile. Mean  $\text{UVA}_{254}$  in ES water (0.56) was nearly three times that of perennial stream water (0.19) suggesting that C was lost or diluted during transport. The ratio of DON:DOC was highest in precipitation and groundwater and reached minimums in throughfall and mineral soil leachate while being relatively high in the O-horizon. Organic horizon water had the most depleted  $\text{DOC-}\delta^{13}\text{C}$ , and there was a steady enrichment with soil depth (O, A, to groundwater). The DON:DOC had a relatively small standard error among potential sources and, hence, is probably a good tracer of DOM in stream water. On the other hand, the stable isotopic composition of DOC varied  $<2\text{‰}$  among stream water and  $<4\text{‰}$  among potential sources; therefore, DOC is indistinguishable from potential sources using stable isotopic signature alone (Table 2). Ephemeral stream DON:DOC and %OC was consistently lower than that of the perennial stream and most closely resembled that of O-horizon leachate, except within the disturbed clear-cut site in which DON:DOC resembled that of mineral soil. Perennial stream DON:DOC was similar to that of groundwater and precipitation. The POC:DOC was similar for ES and perennial stream waters; however, %OC of the perennial stream was significantly higher ( $p = 0.002$ ) than that of ES. Mean ES  $\text{PON-}\delta^{15}\text{N}$  was 1.4 (ranged 0.9 to 2.0) as compared to 1.0 in perennial stream water (Table 2). The PON:POC was similar among streams.

We calculated the area-weighted average instantaneous flux for all storms over the water year. Instantaneous flux is the flow-weighted flux at a given time within an event; thus, instantaneous flux could represent a point on the rising limb, peak flow, or the receding limb of an event. Values represent the means for all events in which we were able to collect water samples and quantify Q with rating curves (Table 3). Average Q was higher in the perennial stream than in the ES (Table 1); however, area-weighted discharge (Unit Q) in the ES was more than twice that of the downstream perennial stream (Table 3), even though the overall area was the same for the ES and perennial streams. Event sampling in ES was triggered by a 20 mm increase in flow over 15 min; thus, the Unit Q measurements only represent periods of high flow (storms) in the ES. There was higher Unit Q from the ES than at the downstream perennial stream gauge suggesting that some of the water discharged to the perennial stream was lost to groundwater before exiting the perennial stream gauge.

**Table 3.** Area-weighted average instantaneous flux of selected surface water constituents.

		Unit Q		TSS		POC		PN		DOC		DON	
		$(\times 10^3 \text{ m}^3 \text{ s}^{-1} \text{ ha}^{-1})$				$(\text{g s}^{-1} \text{ ha}^{-1})$							
A	Ephemeral	12.6	(26)	3432.1	(7285)	99.6	(307)	7.6	(18)	207.6	(589)	13.5	(41)
	Perennial	5.7	(9)	530.1	(1412)	21.8	(36)	2.1	(4)	96.3	(167)	4.5	(9)
B	Ephemeral	−5.7	(1.7)	−0.6	(2.1)	−4.1	(1.9)	−6.4	(1.8)	−3.5	(2.0)	−6.3	(2.1)
	Perennial	−7.6	(3.3)	−3.8	(3.6)	−6.3	(3.5)	−8.7	(3.4)	−5.0	(3.6)	−7.7	(3.1)

Means of unit Q and constituents were computed from within-event samples collected over an entire water year. Values in parentheses are one standard deviation of the mean. Some data were not normally distributed, so we present un-transformed data (A) and log-transformed data (B).

The ES exports were 2.0–6.5 times that of the perennial stream, depending upon the parameter (Table 3). Unit Q was higher for the ephemeral streams as a result of this value being calculated from the sample set from which the constituents were determined. The ephemeral catchments are very small—from 1.8–3.8 ha; yet during storms, their exports were significant which has implications for changes in storm events due to the climate forcing. Surface water, groundwater, and soil storage water are linked, so we used geochemical signatures from the stream exports and potential source areas in order to understand how the pools and fluxes might interact with changes in climate.



### 3.2. Source of OM in Surface Waters during Storms: Active and Contributing Areas

In order to get a better understanding of whether ephemeral and perennial stream waters were derived from similar source areas and were therefore connected during storm events, we compared the CI and UVA<sub>254</sub> of ephemeral and perennial stream event water to that of groundwater and soil leachate. CI was used as a conservative tracer of potential contributors to stream water and UVA<sub>254</sub> was used as a first-order evaluation of DOC inputs. We used UVA<sub>254</sub> rather than DOC because of the strong linear correlation between the two in our data and because the larger UVA<sub>254</sub> dataset gave us better control on variability. The UVA<sub>254</sub> and CI had a significant negative correlation ( $R = -0.595$ ,  $p < 0.001$ ) such that during an event, UVA<sub>254</sub> was elevated and CI concentration was depleted with respect to base flow conditions. The relationship between CI and UVA<sub>254</sub> amongst pools suggests that ES CI and DOC are controlled by water routing through the soil profile, whereas the perennial stream is influenced by groundwater inputs.

We did not attempt to quantify the relative contributions of groundwater versus Horton- and Dunne-type overland flow; however, we used OM characteristics of ES and potential source areas to clarify from which pools ES water may have been derived (Figures 3 and 4). We did not attempt to trace N through the system; however, N and C cycling are coupled therefore we incorporated both components in source-attribution, and the ensuing discussion is framed in terms of OM. Ephemeral storm water DOC- $\delta^{13}\text{C}$  was intermediate between that of groundwater and soil solution dissolved OM with a DON:DOC composition close to that of soil solution and the *minimum* DON:DOC value (max N:C value) for groundwater (Figure 3).

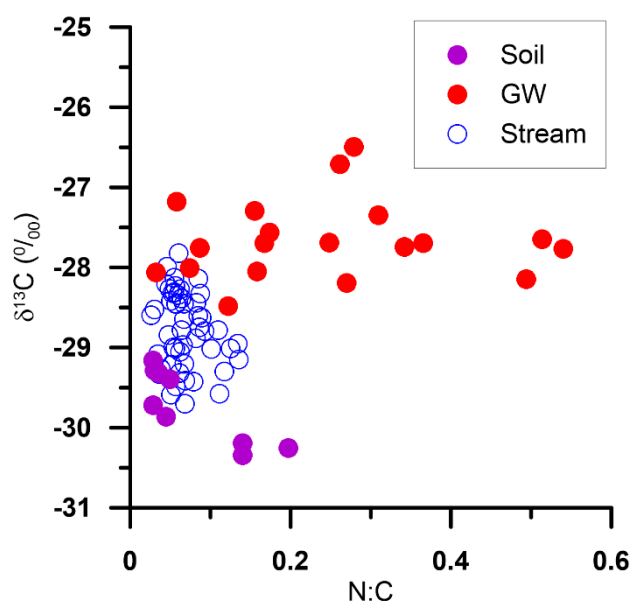


**Figure 3.** Relationship of N:C and  $\delta^{13}\text{C}$  of DOM from groundwater, soil lysimeter, and ephemeral stream event water. Lysimeter samples were collected from below the litter layer, 10 cm into mineral soil, and 20 cm into mineral soil (undifferentiated in this plot).

A comparison between DOM and suspended sediment particulate organic matter (POM) of ES collected during storm events (Figure 4) illustrates the difference in source attributes for DOM and POM. Ephemeral stream DOM and suspended sediment POM clustered tightly in separate- $\delta^{13}\text{C}$  versus N:C mixing spaces: storm water plotted in a space that was close to intermediate soil dissolved OM values, whereas suspended sediment particulate DOM plotted closest to values of A- and B-horizon mineral soils (Figure 4a). Soil leachate values plotted close to that of O-horizon POM (and to a lesser extend A-horizon POM) suggesting that O-horizon soils were an accessible source for labile DOM during storm events. Workers have reported that as much as 66% of DOC in stormflow from

headwater streams originated as saturated flow through the uppermost soil horizons within the riparian zone [50]. Estimated contributions from the upper portions of the soil profile (for lowland riparian soils) represent 64–86% of DOC flux in some watersheds (e.g., [51]). High DOC values were attributed to a larger proportion of wetland soils (i.e., larger potential DOC pool) and larger watershed area [51]. Storm-derived ES POM was more closely related to A-horizon and to a lesser extent B-horizon soils (Figure 4a–c), which suggests that these soils are mobilized or reworked enough to release POM during storm events.

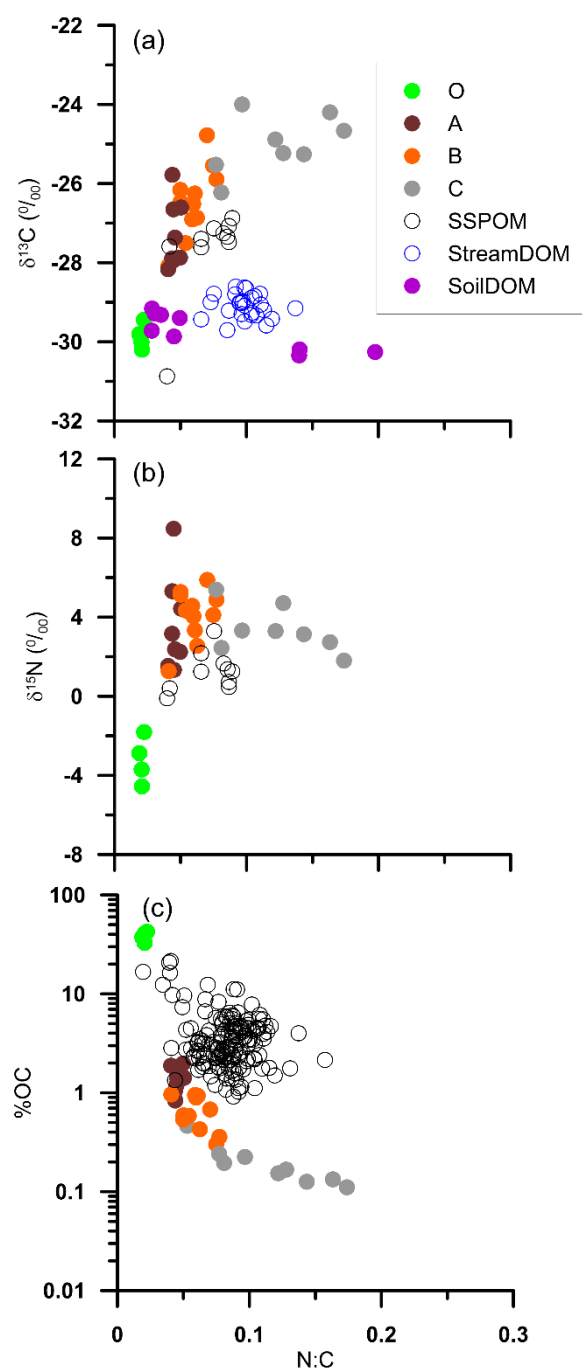


**Figure 4.** N:C versus (a)  $\delta^{13}\text{C}$  of stream DOM, soil solution DOM, POM from soils (O, A, B, C horizons), suspended sediment (SSPOM); (b)  $\delta^{15}\text{N}$ ; and (c) %OC by mass. Stream DOM and suspended sediment POM values are for ES event samples only. In Figure 5a, purple circles with lower N:C represent DOM from A-horizon lysimeters; purple circles with higher N:C represent DOM from O-horizon lysimeters.

### 3.3. Storm-Driven C Dynamics

Samples collected during storm events provided evidence that the ES interacted with the soil profile during rainfall events. The next question we wanted to answer was whether the source or proportion of sources changed within a storm event. We selected storm events for which there was sufficient data to construct plots illustrating the behavior of TSS and OM over the course of an event (Figure 5). The TSS concentrations in ES were highest at the start of an event before peak Q and declined as the event progressed (Figure 5a). Peak perennial stream TSS concentration lagged behind ES peak TSS and coincided with an initial increase in Q. The N:C of particulate material remained constant as ES TSS decreased throughout an event (Table 2 and Figure 5b), thus there is a separation of C-poor material and C-rich material as the event progresses. There is a weak trend of enrichment in  $\delta^{13}\text{C}$  with event time (Figure 5c) which suggests a within-event shift in C to progressively deeper sources.

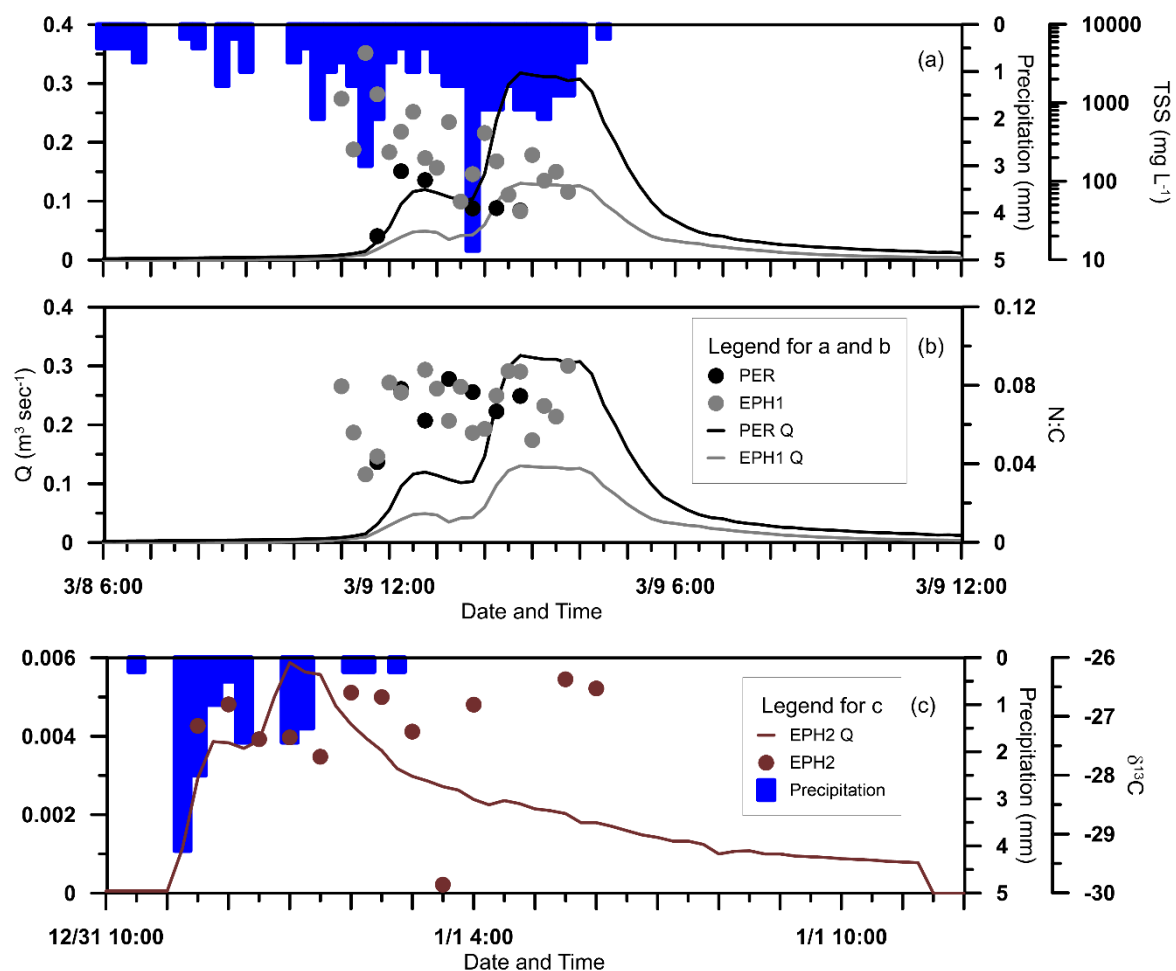


**Figure 5.** Representative behavior of suspended sediment and POC during selected storm events. Blue bars are precipitation amounts. Solid lines indicate within-storm Q. Circles indicate measured values of discrete samples. PER = perennial stream. EPH = ephemeral stream. (a) Suspended Sediment (b) N:C of POM in suspended sediment (c) Change in  $\delta^{13}\text{C}$  of POM in suspended sediment. Sampling start and stop times were controlled by preset criteria (see methods) and thus do not span the time range from start of precipitation to return to base flow. The single anomalously low  $\delta^{13}\text{C}$  value may be due to entrainment of a piece of fresh leaf litter.

We attempted to track the responses of UVA<sub>254</sub> (as a proxy for DOC) and Cl to storms in the perennial and ephemeral watersheds by constructing hysteresis plots from each of the 5 potential sources. In general, we found that the ES (31 December 2010, 30 April 2010, and 4 April 2011 storm

panels in Figure 6) had higher  $\text{UVA}_{254}$  and lower Cl than the perennial stream (23 April 2010 storm panel). However, there were different trends among watersheds and storms.

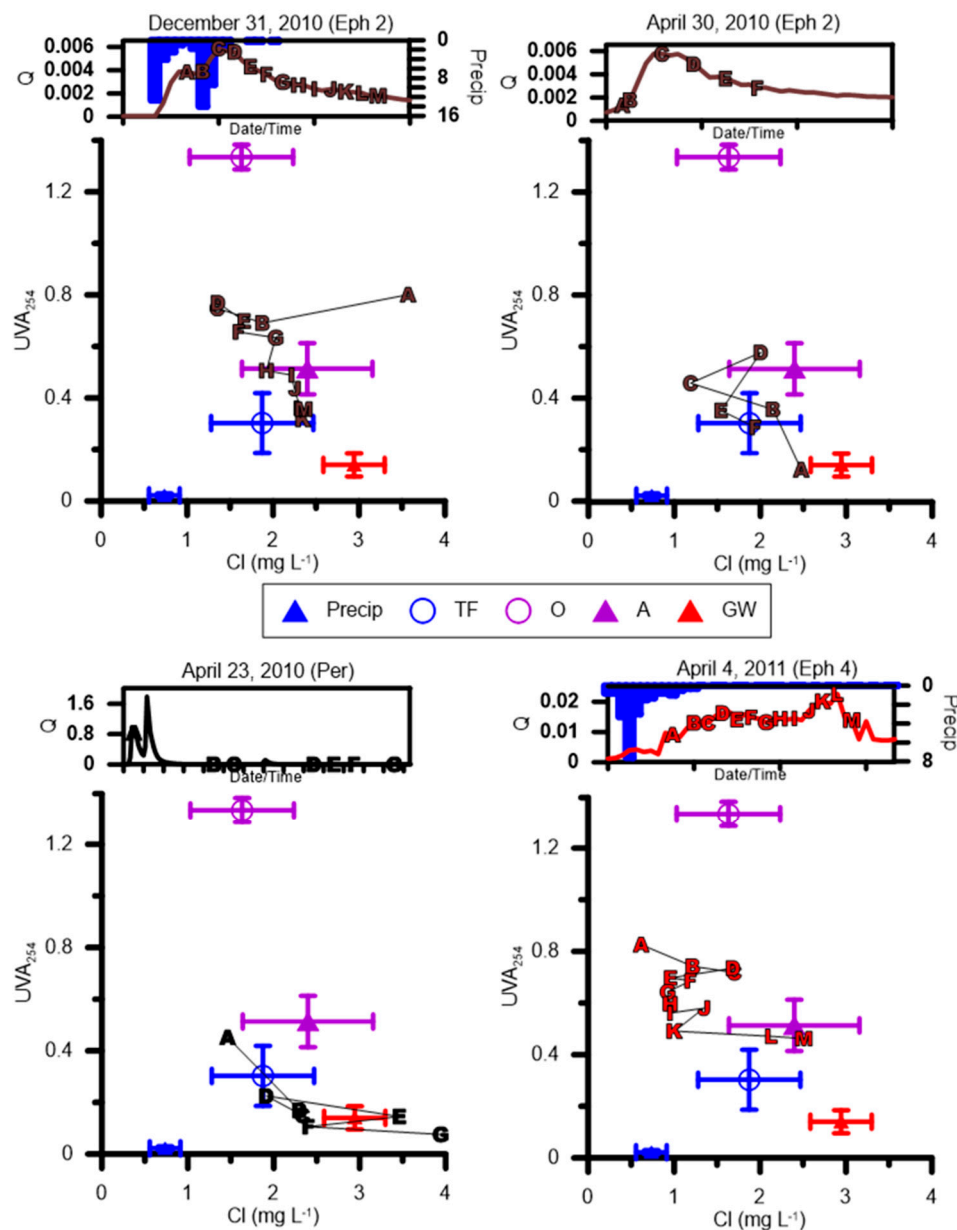


**Figure 6.** Selected (typical) responses of  $\text{UVA}_{254}$  versus Cl concentration for several storms. The date of each event is listed above each pair of plots. Major ticks on the date/time axis of storm discharge plots are spaced every 3 h. The top plot of each pair includes a box inset with hydrographs (line representing Q with scale on left) and precipitation where available (bars with scale on right). Hydrographs are color-coded as to the catchment: brown = ephemeral 2; red = ephemeral 4; black = perennial. Precipitation data for April 23 and April 30 do not exist. Below the hydrograph insets, samples for a given event are plotted on a UVA versus Cl plot. Plots of  $\text{UVA}_{254}$  versus Cl are in alphabetical order by time stamp of sample collection. Letters represent the time point when a sample was collected (in alphabetical order by time stamp of sample collection); corresponding letters on the hydrograph and the UVA–Cl plot are the same sample. Within the plot sample schema: solid blue triangles are precipitation (precip), unfilled blue circles are throughfall (TF), unfilled purple circles are O-horizon leachate (O), solid purple triangles are A horizon leachate (A), and solid red triangles are groundwater samples (GW) (see legend in the center of the figure). Sources are average  $\pm$  95% confidence intervals of samples collected throughout the entire study.



An early season storm (31 December 2010) showed what appears to be flushing of a high Cl and UVA<sub>254</sub> source that could be recently fallen litter. Cl concentration becomes diluted as the source of stream water shifted towards throughfall and then a mixture of O-horizon leachate and precipitation. The source then shifted towards throughfall and A-horizon leachate and eventually towards the groundwater source.

This pattern essentially repeats itself in a later season storm (30 April 2010) in the same watershed (ES2) without the flushing of recently fallen litter. For a late spring storm (4 April 2011) in ES4 (clearcut), there appears to be less influence from throughfall on the earliest storm samples, but the source of water eventually shifts through the soil and towards groundwater. The source of water from the perennial stream (23 April 2010) appears to be from deeper within the soil profile at the onset of a typical storm event relative to the ES. Eventually the source of water appears to be entirely derived from a groundwater source late in the event.

Differences in hysteresis at different times of the year suggest that there may be critical thresholds in some storm parameters that control both the source from which the sediment and OM are derived and the flux of sediment and OM within the system. Due to our sampling protocol, it is possible that the timing of our sampling in relation to the storm hydrograph varied with season; however, our sampling procedure was designed to eliminate as much bias as possible. We compared surface water characteristics to seven event variables related to storms: discharge, peak time, flow time, rate of change, event time, water year day, and precipitation (Table 4) to glean which event variables exerted the greatest control over surface water concentrations and fluxes in ES and perennial streams. Where distributions were not normal, we log-transformed the data. Data presented are those that were significant predictors of constituent flux. The larger the value, the greater the control. The sign determines whether the event variable was negatively or positively associated with the dependent variable.

**Table 4.** Significance of relationships among event variables and selected surface water characteristics of ephemeral streams (ES) and the perennial stream (PER).

		Precipitation		Q		Peak Time		Flow Time		Rate Change		Event Time		WY Day		R <sup>2</sup>
		SC	SE	SC	SE	SC	SE	SC	SE	SC	SE	SC	SE	SC	SE	
TSS	ES	0.300	0.051	1.014	0.115	0.049	0.126	−0.005	0.131	0.065	0.066	−0.209	0.064	0.225	0.057	0.664
	PER	−0.205	0.073	0.468	0.142					0.144	0.065					0.684
POC	ES	0.225	0.044	0.674	0.097			−0.130	0.054			−0.106	0.072	0.111	0.049	0.777
	PER	−0.171	0.052	0.465	0.102					0.117	0.047					0.788
PN	ES	0.248	0.042	0.645	0.080			−0.129	0.047					0.174	0.108	0.805
	PER	−0.329	0.092	0.801	0.179					0.184	0.082					0.796
DOC	ES	0.043	0.032	1.307	0.166	0.324	0.136	−0.291	0.086			−0.179	0.076	−0.117	0.069	0.909
	PER			1.189	0.422											0.581

Standardized coefficients (SCs) and standard error (SE) of predictors that were selected through AIC and stepwise procedures. Dependent variables: Precipitation = amount of precipitation that fell in the previous 15 min; Q = instantaneous discharge at the time the sample was collected; PeakTime = time before or after peak flow; FlowTime = time since flow began in hours; RateChange = change in Q over time where positive values are on the rising limb and negative values are on the receding limb; EventTime = time since event initiation; WY Day = # of days after 1 October (beginning of water year). Q, TSS, POC, PN, and DOC were all log-transformed to meet assumptions of normality.

As expected, Q and precipitation exerted the greatest control on TSS and OM for both streams. Precipitation is interesting in that all of the measured exports of ES increased with increasing precipitation, whereas the reverse was true in the perennial stream either as a result of dilution of exports as they reached the perennial stream or reduced carrying capacity in the perennial stream, or both. An increase in DOC with increasing precipitation and Q has been reported in other headwater studies (e.g., [26]). Rate Change, which is tied to the shape of the hydrograph (i.e., flashy behavior equates to a more rapid rate of change), was a significant predictor for TSS, POC, and PN in the perennial stream, but was weakly correlated to TSS in the ES. The other independent variables, PeakTime, FlowTime, EventTime, and WY DAY, were significant only for ES. Dependent variables decreased with increasing FlowTime and EventTime, which suggests that there was a pool of sediment, DOM, and POM which was accessed early in an event and became depleted over time. The positive

correlation with WY DAY for all dependent variables indicates that the time at which the pools were accessed may be significant in terms of interpreting potential responses to climate change. We recognize that WY DAY likely has a sinusoidal relationship and, thus, may not be a good predictor; however, we explored the use of sin transformation and it did not improve  $R^2$ .

### 3.4. The Water Year

There is a growing body of evidence that the seasonal component to OM pools and fluxes in headwater streams (e.g., [24]) is linked to the wet–dry cycles that are prevalent in IRES and affects the quality and quantity of OM exports from IRES (e.g., [26,30,52,53]). If that is the case, then there should be a relationship between flux and timing within the water year, as the watershed transitions from hot, dry summer conditions to cool, wet winter conditions. We examined correlations between dissolved and particulate constituents and timing within the water year (WY Day; 1 October to 30 September) to see if there were effects associated with wet and/or dry periods (Table 4). There were significant effects between WY Day and flux of TSS, POC, PN, and DOC for ES, whereas these fluxes were not significant for the perennial stream. Flux of TSS, POC, and PN all had positive correlations with WY Day which indicates that flux of these particulates increases over the course of the water year. The most likely mechanism for this would be active downcutting and headward erosion which releases sediment and associated particulate OM into ES with successive storm events.

The negative correlation between water year date versus DOC indicates that ES DOC concentration was highest at the beginning of the “wet” season and gradually decreased over time which is consistent with data from a meta-analysis of 30 forested watersheds in the eastern United States documenting higher DOC exports at the end of a dry period [26]. Flushing of high CI and UVA<sub>254</sub> sources (e.g., throughfall and O-horizon material; Table 2) during an early season storm (Figure 6; 31 December 2010 storm panel) is not as evident later in the season. The late season storm (Figure 6; 30 April 2010 storm panel) has a CI versus UVA<sub>254</sub> signal which is similar to GW (i.e., wet season base flow) at the event onset, followed by throughfall and A-horizon soil. These relationships suggest that early in the season there was a larger pool of labile DOC available within and leached from the upper soil profile (e.g., O-horizon soil solution) and that over multiple flushing events the labile C pool was depleted. If storm events are “hot moments” for the flushing of stored DOC [28,40], then peak DOC efflux should occur at the onset of the wet season (late fall) and decrease throughout the wetter winter months during successive leaching events. The DOC pool will build during drier months such that events that occur after prolonged dry conditions will have high DOC concentrations [26,54]. Our data support belowground storage of a leachable C pool during the dry season and flushing of the soil C pool during storm events throughout the wet season, such that availability of DOC decreases to minimum at the beginning of the next dry season. In contrast, the flushing signal that is evident within the ES is not detectable within the perennial stream, most likely due to the dilution from groundwater inputs (Figure 6; 23 April 2010) or CO<sub>2</sub> evasion.

### 3.5. The Climate Connection

Climate projections for the southeastern US indicate a slight increase in warm days and especially warm nights, which will lead to a longer duration of frost-free days, and an increase in drought length [55]. Concurrent with the overall increase in temperature, there is “high confidence” that there will be an increase in the number of annual days for which there are heavy (>75 mm) precipitation events [55] even though MAP is expected to be relatively stable [34]. A comparison of several models from the Mississippi River Basin also predict an increase in temperature which leads to a shift in the seasonality of the precipitation such that precipitation will decrease during summer months and increase during winter months [56]. Regional climate models from the central U.S. postulate a localized summertime warming minimum or “warming hole” [57] such that convective storms will result in precipitation that is greater than evapotranspiration, setting the stage for increases in soil moisture at

the end of the summer season. These models pose a conundrum for how climatic drivers will affect fluxes from IRES to downstream rivers.

If MAP does not change but event precipitation increases, then there must be less frequent events of higher intensity with increased drying time between events. This scenario would result in higher fluxes of Sediment and OM (until it is depleted seasonally) from the ephemeral watersheds with increasing precipitation and Q (Table 4) especially during the first flood pulses as has been reported for both particulate and dissolved OM e.g., [5,26]. The four ephemeral watersheds we gauged had a combined area of 11.6 ha, representing 36% of the source area contributing to the perennial stream at our gauge point, yet as small as they were, they discharged an average of  $328 \text{ g s}^{-1} \text{ ha}^{-1}$  of OM (Table 3; POC + PN + DOC + DON) during storm events. The high standard deviations of these measurements indicate that the fluxes could be much higher or much lower. We used the existing relationship between precipitation/Q and the dependent variables within a regression function to provide an indication of how the watershed might respond to increases in precipitation or Q. The equation used was:

$$\begin{aligned} \ln(X) = B0 + B1 & * \ln(\text{unit}Q) + B2 * (\text{Peak time}) + B3 * (\text{Flowtime}) + B4 \\ & * (\text{Rate of Change}) + B5 * (\text{TimeEvent}) + B6 * (\text{WY Day}) + B7 \\ & * (\text{Precip}) \end{aligned}$$

where X is the dependent variable of interest (e.g., TSS, POC, PN, and DOC), B0 is the intercept, and B1–B7 are the coefficients for each of the predictor variables (0 if the predictor variable was not a significant predictor of the dependent). The resultant projected increase or decrease (%) in TSS and OM components given a 5% increase in precipitation or Q is provided in Table 5.

**Table 5.** Projected increase in TSS and OM components with 5% increase in precipitation or Q and coefficients from which they were derived.

		Q	Precipitation	Peak Time	FlowTime	Rate Change	TimeEvent	WY Day	5% Δ in Precip	5% Δ in Q
TSS	ES	0.408	0.297				−0.211	0.237	2.0	2.0
	PER	0.320	−0.221			4.197			−4.6	1.6
POC	ES	0.388	0.103		−0.012		−0.064	0.003	0.7	1.9
	PER	0.484	−0.268			5.040			−5.4	2.4
PN	ES	0.349	0.131		−0.015			0.007	0.9	1.7
	PER	0.551	−0.349			5.196			−7.0	2.7
DOC	ES	0.563	−0.003	0.018	−0.007		−0.040	−0.003	0.0	2.8
	PER	0.466							0.0	2.3

Projected increase or decrease in each of the dependent variables are in percentage in the two columns to the right. ES = ephemeral streams. PER = perennial stream. Dependent variables: Precipitation = amount of precipitation that fell in the previous 15 min; Q = instantaneous discharge at the time the sample was collected; PeakTime = time before or after peak flow; FlowTime = time since flow began in hours; RateChange = change in Q over time where positive values are on the rising limb and negative values are on the receding limb; EventTime = time since event initiation; WY Day = # of days after October 1 (beginning of water year).

A century-long study of precipitation trends in forest lands of the Lower Mississippi River Alluvial Valley (LMRAV) reported precipitation increases (estimated to be 7%) at the south coastal area of the LMRAV and constant or a slight decrease at the middle area of the LMRAV [58]. Our study site was between the south and middle parts of the LMRAV and, therefore, a 5% increase in precipitation is a reasonable estimate. A 5% increase in stream discharge is considered as the extreme case because not all of the 5% increase precipitation contributes to discharge.

Where there is a 5% increase in precipitation, within ES we would expect increases across all particulate constituents. However, given the perennial stream sensitivity to precipitation there would most likely be a negative effect of on the flux of most constituents. When and how the precipitation occurs can change the outcome insofar as precipitation and Q are coupled. Higher magnitude storms, which may cause an increase in Q, will be the primary drivers for additional materials flux. Given a 5% increase in Q, there was an increase from 1.6% to 2.8% in average instantaneous flux of materials

from both the ES and the perennial stream (Table 5). For example, an increase of  $0.63 \times 10^3 \text{ m}^3 \text{ s}^{-1} \text{ ha}^{-1}$  in  $Q$  within ES would result in an increase of  $69.0 \text{ g s}^{-1} \text{ ha}^{-1}$  average instantaneous flux of TSS and  $7.8 \text{ g s}^{-1} \text{ ha}^{-1}$  of OM (Table 6). While increases appear to be small, it is important to remember these are instantaneous fluxes, so over the course of an event the flux will be much higher depending upon the change in the discharge-rating curve relative to historical data. Changes between ES and the perennial stream are similar, which suggests that materials flux from the ES continues in the perennial stream and that the perennial stream acts as a conduit for materials generated in the ES.

**Table 6.** Modeled increase in average within-event instantaneous flux of materials given a 5% increase in  $Q$ .

	5% $\Delta$ Unit $Q$ ( $\times 10^3 \text{ m}^3 \text{ s}^{-1} \text{ ha}^{-1}$ )	$\Delta$ TSS	$\Delta$ POC	$\Delta$ PN	$\Delta$ DOC	$\Sigma$ OM
		(g s <sup>-1</sup> ha <sup>-1</sup> )				
Ephemeral	0.63	69.00	1.90	0.13	5.78	7.82
Perennial	0.28	8.34	0.52	0.06	2.22	2.79

Instantaneous flux is  $Q \times C$ , where  $Q$  is the instantaneous discharge and  $C$  is the concentration of the sample at the time of sample collection.

The hydrologic transition from dry to wet in these IRES could result in pulses of DOC release [30,31,59] followed by mineralization and  $\text{CO}_2$  release from the perennial stream [60], especially since rates increase with increasing catchment area [61]. Much of the DOC and POC in the ES derived from the soil profile (Figures 2 and 3). If, as a result of climate change, there is an increase in convective storms and greater soil moisture at the end of the summer season, then wetting and drying cycles of soils and streams will be moderated and there may be lower DOC production and flux simultaneously with higher POM due to the increased energy in the system to mobilize particulates and sediment.

If MAP does not change but rainfall shifts to winter months, then presumably the summer drought season would be lengthened. Increased drought during the warmer months followed by short-term high intensity events would result in increased downcutting and headward erosion followed by greater flux of TSS, POC, and PN (Figure 4 and Table 3). A compilation of climate models for an agricultural watershed in Mississippi predicted that an increase in summer temperatures would result in a decrease in runoff, but approximately 12% greater TSS loads, presumably due to the higher intensity precipitation events [62]. Perhaps of greater import is that prolonged drought may increase the areal extent of IRES [1] which means that there would be a greater time and area over which soil OM can accumulate. If Horton infiltration excess is the primary path for DOC to streams, then perhaps there would be no change beyond what is mobilized with sediment due to the erosion. If Dunne saturation excess is the primary source of DOC as is suggested by our data (Figures 2 and 4a), then there will be a greater time over which the pool can build and potentially larger releases to the stream network. Longer-term studies are needed to determine the impact of climate change on the flux of (OM) from IRES in the southeastern US.

#### 4. Conclusions

Our first question was: what are the sources of sediment and OM in ES? DOM was derived from Dunne-type saturated flow through the upper part of the soil profile, particularly during the first flush of storms and after dry periods. Sediment and POM were derived from down cutting and headward erosion during the rising limb of storm events. Changes in processes that affect erosion are going to lengthen stream channel networks and increase the areal extent of ES.

Our second question was: what are the controls on flux of sediment and OM from very small (<4 ha) ES to downstream reaches? Precipitation, WY Day, and variables associated with the shape of the hydrograph all had linear relationships with sediment, DOM, and POM. No matter what happens to the other variables (e.g., precipitation, length of the water year, shape of the hydrograph), discharge will have an overriding effect on the flux of materials because there is a power log relationship between



Q and materials flux. Any changes to Q (i.e., caused by higher-intensity storms) will have a large control over the flux.

The flux of OM in response to climate change is going to be dependent upon how the change affects the source of OM. Projected climate effects are: (1) less frequent, higher-intensity storms and/or (2) shift to heavier precipitation in winter and longer drought in summer. If there is a shorter water year but the same amount of precipitation, there needs to be a longer/larger stream network to accommodate the flow. Precipitation during storms is likely to result in more water transfer through the upper part of the soil profile in conjunction with increased channel incision. Higher intensity storms resulting in higher Q within ES channels will result in greater flux of materials to downstream perennial reaches.

Do small IRES matter in the context of climate change? Given the storm-driven flux of sediment and OM from these small ephemeral watersheds and the potential for that OM to be processed and evolved as CO<sub>2</sub> under projected climate scenarios for the region, the answer is yes—IRES matter. There are three reasons that ES should be incorporated into climate-driven hydrological models: (1) ES are intimately connected to sources of OM; (2) ES are indirectly connected to precipitation through Q; (3) there is likely to be an expansion of the areal extent of ES. For these reasons we need to consider ES when modeling the response of hydrological systems to climate change.

**Author Contributions:** Conceptualization, J.D. and J.H.; methodology, J.D., J.H.; B.C., and C.M.; software, J.D. and J.H.; validation, J.D., J.H., B.C., and C.M.; formal analysis, J.H.; investigation, J.D., J.H., B.C., and C.M.; resources, J.D., J.H., and Y.O.; data curation, J.H.; writing—original draft preparation, J.D.; writing—review and editing, J.D., J.H., and Y.O.; visualization, J.D. and J.H.; supervision, J.D. and J.H.; project administration, J.D. and J.H.; funding acquisition, J.D. and J.H. All authors have read and agreed to the published version of the manuscript.

**Funding:** This research was funded by the US Geological Survey through Mississippi Water Resources Research Institute, grant number 06HQGR0094 06090820; the US Department of Agriculture Forest Service, grant number 06JV11330127186 07010040, the National Council for Air and Stream Improvement, Inc., grant number 07030270, and Weyerhaeuser Company, grant number 07100923.

**Acknowledgments:** Mississippi State University Forest and Wildlife Research Center provided laboratory support; Weyerhaeuser Company provided site support. Rick Maiers and the students at the Mississippi State University assisted with the project setup.

**Conflicts of Interest:** The authors declare no conflict of interest.

## References

1. Datry, T.; Corti, R.; Foulquier, A.; von Schiller, D.; Tockner, K. One for all, all for one: A global river research network. *Eos* **2016**, *97*, 12–15. [CrossRef]
2. Acuña, V.; Datry, T.; Barceló, D.; Dahm, C.N.; Ginebreda, A.; McGregor, G.; Sabater, S.; Tockner, K.; Palmer, M.A. Why should we care about temporary waterways? *Science* **2014**, *33*, 1080–1081. [CrossRef] [PubMed]
3. Alexander, L.C.; Autrey, B.; Demeester, J.; Fritz, K.; Goodrich, D.; Kepner, W.G.; Lane, C.R.; LeDuc, S.; Leibowitz, S.; McManus, M.; et al. Connectivity and Effects of Streams and Wetlands on Downstream Waters: A Review and Synthesis of the Scientific Evidence. EPA/600/R-14/475F. January 2015. Available online: <https://nepis.epa.gov> (accessed on 7 July 2020).
4. Gutiérrez-Jurado, K.Y.; Partington, D.; Batelaan, O.; Cook, P.; Shanafield, M. What triggers streamflow for intermittent rivers and ephemeral streams in low-gradient catchments in Mediterranean climates. *Water Resour. Res.* **2019**, *55*, 9926–9946. [CrossRef]
5. Brintrup, K.; Amigo, C.; Fernández, J.; Hernández, A.; Pérez, F.; Félez-Bernal, J.; Butturini, A.; Saez-Carillo, K.; Yevenes, M.A.; Figueroa, R. Comparison of organic matter in intermittent and perennial rivers of Mediterranean Chile with the support of citizen science. *Rev. Chil. Hist. Nat.* **2019**, *92*, 3. [CrossRef]
6. Raymond, P.A.; Saiers, J.E.; Sobczak, W.V. Hydrological and biogeochemical controls on watershed dissolved organic matter transport: Pulse—Shunt concept. *Ecology* **2016**, *97*, 5–16. [CrossRef]
7. Raymond, P.A.; Hartmann, J.; Lauerwald, R.; Sobek, S.; McDonald, C.; Hoover, M.; Butman, D.; Striegl, R.; Mayorga, E.; Humborg, C.; et al. Global carbon dioxide emissions from inland waters. *Nature* **2013**, *503*, 355–359. [CrossRef] [PubMed]

8. Marx, A.; Dusek, J.; Jankovec, J.; Sanda, M.; Vogel, T.; van Geldern, R.; Hartmann, J.; Barth, J.A.C. A review of CO<sub>2</sub> and associated carbon dynamics in headwater streams: A global perspective. *Rev. Geophys.* **2017**, *55*, 560–585. [\[CrossRef\]](#)
9. Fritz, K.M.; Schofield, K.A.; Alexander, L.C.; McManus, M.G.; Golden, H.E.; Lane, C.R.; Kepner, W.G.; LeDuc, S.D.; DeMeester, J.E.; Pollard, A.I. Physical and chemical connectivity of streams and riparian wetlands to downstream waters: A synthesis. *J. Am. Water Res. Assoc.* **2018**, *54*, 323–345. [\[CrossRef\]](#)
10. MacDonald, L.H.; Coe, D. Influence of headwater streams on downstream reaches in forested areas. *For. Sci.* **2007**, *53*, 148–168. [\[CrossRef\]](#)
11. Nadeau, T.; Rains, M. Hydrological connectivity between headwater streams and downstream waters: How science can inform policy. *J. Am. Water Resour. Assoc.* **2007**, *43*, 118–133. [\[CrossRef\]](#)
12. Gomi, T.; Sidle, R.; Richardson, J. Understanding processes and downstream linkages of headwater systems. *Bioscience* **2002**, *52*, 905–916. [\[CrossRef\]](#)
13. Triska, F.; Duff, J.; Sheibley, R.; Jackman, A.; Avanzion, R. DIN retention–transport through four hydrologically connected zones in a headwater catchment of the upper Mississippi River. *J. Am. Water Res. Assoc.* **2007**, *43*, 60–71. [\[CrossRef\]](#)
14. Winterdahl, M.; Bishop, K.; Erlandsson, M. Acidification, dissolved organic carbon (DOC) and climate change. In *Global Environmental Change*; Freedman, B., Ed.; Springer: Dordrecht, The Netherlands, 2014; pp. 281–287.
15. Mengistu, S.D.; Quick, C.G.; Creed, I.F. Nutrient exports from catchments on forested landscapes reveals complex nonstationary and stationary climate signals. *Water Resour. Res.* **2013**, *49*, 3863–3880. [\[CrossRef\]](#)
16. Alveras-Cobelas, M.; Angeler, D.G.; Sanchez-Carillo, S.; Almendros, G. A worldwide view of carbon export from catchments. *Biogeochemistry* **2012**, *107*, 275–293. [\[CrossRef\]](#)
17. Aufdenkampe, A.K.; Mayorga, E.; Raymond, P.A.; Melack, J.m.; Doney, S.C.; Alin, S.R.; Aalto, R.E.; Yoo, K. Riverine coupling of biogeochemical cycles between land, oceans, and atmosphere. *Front. Ecol. Environ.* **2011**, *9*, 53–60. [\[CrossRef\]](#)
18. Tank, J.L.; Rosi-Marshall, E.J.; Griffiths, N.A.; Entekin, S.A.; Stephen, M.L. A review of allochthonous organic matter dynamics and metabolism in streams. *J. N. Am. Benthol. Soc.* **2010**, *29*, 118–146. [\[CrossRef\]](#)
19. Hejzlar, J.; Dubrovsky, M.; Buchtele, J.; Ruzicka, M. The apparent and potential effects of climate change on the inferred concentration of dissolved organic matter in a temperate stream (the Malse River, South Bohemia). *Sci. Total Environ.* **2003**, *310*, 143–152. [\[CrossRef\]](#)
20. Horton, R.E. Erosional development of streams and their drainage basins: Hydrophysical approach to quantitative morphology. *Bull. Geol. Soc. Am.* **1945**, *56*, 275–370. [\[CrossRef\]](#)
21. Dunne, T.; Black, R.D. An experimental investigation of runoff production in permeable soils. *Water Resour. Res.* **1970**, *6*, 478–490. [\[CrossRef\]](#)
22. Hansen, W.F. Identifying stream types and management implications. *For. Ecol. Manag.* **2001**, *143*, 39–46. [\[CrossRef\]](#)
23. Wipfli, M.; Richardson, J.; Naiman, R. Ecological linkages between headwaters and downstream ecosystems: Transport of organic matter, invertebrates, and wood down headwater channels. *J. Am. Water Res. Assoc.* **2007**, *43*, 72–85. [\[CrossRef\]](#)
24. Wilson, H.F.; Saiers, J.E.; Raymond, P.A.; Sobczak, W.V. Hydrologic drivers and seasonality of dissolved organic carbon concentration, nitrogen content, bioavailability, and export in a forested New England stream. *Ecosystems* **2013**, *16*, 604–616. [\[CrossRef\]](#)
25. Hatten, J.A.; Goñi, M.A.; Wheatcroft, R.A. Chemical characteristics of particulate organic matter from a small mountainous river system in the Oregon coast Range, USA. *Biogeochemistry* **2012**, *107*, 43–66. [\[CrossRef\]](#)
26. Raymond, P.A.; Saiers, J.E. Event controlled DOC export from forested watersheds. *Biogeochemistry* **2010**, *100*, 197–209. [\[CrossRef\]](#)
27. Moody, C.S.; Worrall, F.; Evans, C.D.; Jones, T.G. The rate of loss of dissolved organic carbon (DOC) through a catchment. *J. Hydrol.* **2013**, *492*, 139–150. [\[CrossRef\]](#)
28. McClain, M.E.; Boyer, E.W.; Dent, C.L.; Gergel, S.E.; Grimm, N.B.; Groffman, P.M.; Hart, S.C.; Harvey, J.W.; Johnston, C.A.; Mayorga, E.; et al. Biogeochemical hot spots and hot moments at the interface of terrestrial and aquatic ecosystems. *Ecosystems* **2003**, *6*, 301–312. [\[CrossRef\]](#)

29. von Schiller, D.; Graeber, D.; Ribot, M.; Timoner, X.; Acuña, V.; Martí, E.; Sabater, S.; Tockner, K. Hydrological transitions drive dissolved organic matter quantity and composition in a temporary Mediterranean stream. *Biogeochemistry* **2015**, *123*, 429–446. [\[CrossRef\]](#)
30. Vázquez, E.; Ejarque, E.; Ylla, I.; Romaní, A.M.; Butturini, A. Impact of drying/rewetting cycles on the bioavailability of dissolved organic matter molecular-weight fractions in a Mediterranean stream. *Freshw. Sci.* **2015**, *34*, 263–275. [\[CrossRef\]](#)
31. Vázquez, E.; Romaní, A.M.; Sabater, F.; Butturini, A. Effects of the dry–wet hydrological shift on dissolved organic carbon dynamics and fate across stream–riparian interface in a Mediterranean catchment. *Ecosystems* **2007**, *10*, 239–251. [\[CrossRef\]](#)
32. Gómez-Gener, L.; Obrador, B.; Marcé, R.; Acuña, V.; Catalán, N.; Casas-Ruiz, J.P.; Sabater, S.; Muñoz, I.; von Schiller, D. When water vanishes: Magnitude and regulation of carbon dioxide emissions from dry temporary streams. *Ecosystems* **2016**, *19*, 710–723. [\[CrossRef\]](#)
33. Benstead, J.P.; Leigh, D.S. An expanded role for river networks. *Nat. Geosci.* **2012**, *5*, 678–679. [\[CrossRef\]](#)
34. Karl, T.R.; Melillo, J.M.; Peterson, T.C. (Eds.) *Global Climate Change Impacts in the United States*; Cambridge University Press: New York, NY, USA, 2009.
35. Haarsma, R.J.; Hazeleger, W.; Severijns, C.; de Vries, H.; Sterl, A.; Bintanja, R.; van Oldenborgh, G.J.; van den Brink, H.W. More hurricanes to hit western Europe due to global warming. *Geophys. Res. Lett.* **2013**, *40*, 1783–1788. [\[CrossRef\]](#)
36. Knutson, T.R.; McBride, J.L.; Chan, J.; Emanuel, K.; Holland, G.; Landsea, C.; Held, I.; Kossin, J.P.; Srivastava, A.K.; Sugi, M. Tropical cyclones and climate change. *Nat. Geosci.* **2010**, *3*, 157–163. [\[CrossRef\]](#)
37. Yoon, B.; Raymond, P.A. Dissolved organic matter export from a forested watershed during hurricane Irene. *Geophys. Res. Lett.* **2012**, *39*, L18402. [\[CrossRef\]](#)
38. Wheatcroft, R.A.; Goñi, M.A.; Hatten, J.A.; Pasternack, G.B.; Warrick, J.A. The role of effective discharge in the ocean delivery of particulate organic carbon by small, mountainous river systems. *Limnol. Oceanogr.* **2010**, *55*, 161–171. [\[CrossRef\]](#)
39. Nash, D.B. Effective Sediment-Transporting Discharge from Magnitude-Frequency Analysis. *J. Geol.* **1994**, *102*, 79–95. [\[CrossRef\]](#)
40. Vidon, P.; Allan, C.; Burns, D.; Duval, T.P.; Gurwick, N.; Inamdar, S.; Lowrance, R.; Okay, J.; Scott, D.; Sebestyen, S. Hot spots and hot moments in riparian zones: Potential for improved water quality management. *J. Am. Water Resour. Assoc.* **2010**, *46*, 278–298. [\[CrossRef\]](#)
41. Leigh, C.; Boulton, A.J.; Courtwright, J.L.; Fritz, K.; May, C.L.; Walker, R.H.; Datry, T. Ecological research and management of intermittent rivers: An historical review and future directions. *Freshw. Biol.* **2015**, *61*, 1181–1199. [\[CrossRef\]](#)
42. Mangum, C. Flux and Source of Dissolved Organic and Inorganic Constituents in Managed Headwaters of the Upper Gulf Coastal Plain, Mississippi. Master's Thesis, Mississippi State University, Starkville, MS, USA, 2012.
43. McMullen, J.W.; Ford, J.G. Soil Survey of Webster County Mississippi. In *Cooperation with the Mississippi Agricultural and Forestry Experiment Station*; Natural Resources Conservation Service, United States Department of Agriculture: Washington, DC, USA, 1978; 99p.
44. Choi, B.; Dewey, J.C.; Hatten, J.A.; Ezell, A.W.; Fan, Z. Changes in vegetative communities and water table dynamics following timber harvesting in small headwater streams. *For. Ecol. Manag.* **2012**, *281*, 1–11. [\[CrossRef\]](#)
45. U.S. Geological Survey. *Little Sand Creek Quadrangle, Mississippi. 1:24,000; 7.5 Minute Series*; United States Department of the Interior: Reston, VA, USA, 1983.
46. Choi, B.; Hatten, J.A.; Dewey, J.C.; Otsuki, K.; Cha, D. Effect of timber harvesting on stormflow characteristics in headwater streams of managed, forested watersheds in the Upper Gulf Coastal Plain of Mississippi. *J. Fac. Agric. Kyushu Univ.* **2013**, *58*, 395–402.
47. National Climatic Data Center. Eupora 2E, MS, US, Precipitation 15 Minute Station Details. NOAA National Centers for Environmental Information. 2013. Available online: [http://www.ncdc.noaa.gov/cdo-web/datasets/PRECIP\\_15/stations/COOP:222896/detail](http://www.ncdc.noaa.gov/cdo-web/datasets/PRECIP_15/stations/COOP:222896/detail) (accessed on 16 October 2015).
48. R Core Team. *R: A Language and Environment for Statistical Computing*; R Foundation for Statistical Computing: Vienna, Austria, 2017. Available online: <https://www.R-project.org/> (accessed on 10 August 2017).

49. Venables, W.N.; Ripley, B.D. *Modern Applied Statistics with S*, 4th ed.; Springer: New York, NY, USA, 2002; ISBN 0-387-95457-0. Available online: <http://www.stats.ox.ac.uk/pub/MASS4> (accessed on 10 August 2017).
50. Lambert, T.; Pierson-Wickmann, A.-C.; Gruau, G.; Thibault, J.-N.; Jaffrezic, A. Carbon isotopes as tracers of dissolved organic carbon sources and water pathways in headwater catchments. *J. Hydrol.* **2011**, *402*, 228–238. [[CrossRef](#)]
51. Morel, B.; Durand, P.; Jaffrezic, A.; Gruau, G.; Molenat, J. Sources of dissolved organic carbon during stormflow in a headwater agricultural catchment. *Hydrol. Process* **2009**, *23*, 2888–2901. [[CrossRef](#)]
52. Shumilova, O.; Zak, D.; Datry, T.; von Schiller, D.; Corti, R.; Foulquier, A.; Obrador, B.; Tocknet, K.; Allan, D.C.; Altermatt, F.; et al. Simulating rewetting events in intermittent rivers and ephemeral streams: A global analysis of leached nutrients and organic matter. *Glob. Chang. Biol.* **2019**, *25*, 1591–1611. [[CrossRef](#)] [[PubMed](#)]
53. Corti, R.; Datry, T. Invertebrates and sestonic matter in an advancing wetted front travelling down a dry river bed (Albarine, France). *Freshw. Sci.* **2012**, *31*, 1187–1201. [[CrossRef](#)]
54. Johnson, M.S.; Lehmann, J.; Selva, E.C.; Abdo, M.; Riha, S.; Couto, E.G. Organic carbon fluxes within and stream exports from headwater catchments in the southern Amazon. *Hydrol. Process* **2006**, *20*, 2599–2614. [[CrossRef](#)]
55. Carter, L.; Terando, A.; Dow, K.; Hiers, K.; Kunkel, K.E.; Lascrain, A.; Marcy, D.; Osland, M.; Schramm, P. Southeast. In *Impacts, Risks, and Adaptation in the United States: Fourth National Climate Assessment*; Reidmuller, D.T., Avery, C.W., Easterling, D.R., Kunkel, K.E., Lewis, K.L.M., Maycock, T.K., Stewart, B.C., Eds.; U.S. Global Change Research Program: Washington, DC, USA, 2017; Volume II, pp. 743–808. [[CrossRef](#)]
56. Pan, Z.; Zhang, Y.; Liu, X.; Gao, Z. Current and future precipitation extremes over Mississippi and Yangtze River Basins as simulated in CMIP5 models. *J. Earth Sci.* **2016**, *27*, 22–36. [[CrossRef](#)]
57. Pan, Z.; Arriitt, R.W.; Takle, E.S.; Gutowski, W.J., Jr.; Anderson, C.J.; Segal, M. Altered hydrologic feedback in a warming climate introduces a “warming hole”. *Geophys. Res. Lett.* **2004**, *31*, L17109. [[CrossRef](#)]
58. Ouyang, Y.; Zhang, J.; Feng, G.; Wan, Y.; Leininger, T.D. A century of precipitation trends in forest lands of the Lower Mississippi River Alluvial Valley. *Sci. Rep.* **2020**, *10*, 12802. [[CrossRef](#)]
59. Lundquist, E.J.; Jackson, L.E.; Scow, K.M. Wet-dry cycles affect dissolved organic carbon in two California agricultural soils. *Soil Biol. Biochem.* **1999**, *31*, 1031–1038. [[CrossRef](#)]
60. Hotchkiss, E.R.; Hall, R.O., Jr.; Sponseller, R.A.; Butman, D.; Klaminder, J.; Laudon, H.; Rosvall, M.; Karlsson, J. Sources of and processes controlling CO<sub>2</sub> emissions change with the size of streams and rivers. *Nat. Geosci.* **2015**, *8*, 696–699. [[CrossRef](#)]
61. Datry, T.; Foulquier, A.; Corti, R.; von Schiller, D.; Tockner, K.; Mendoza-Lera, C.; Clement, J.C.; Gessner, M.O.; Moleón, M.; Stubbington, R.; et al. A global analysis of terrestrial plant litter dynamics in non-perennial waterways. *Nat. Geosci.* **2018**, *11*, 497–503. [[CrossRef](#)]
62. Yasarer, L.M.W.; Bingner, R.L.; Garbrecht, J.D.; Locke, M.A.; Lizotte, R.E., Jr.; Momm, H.G.; Busteed, P.R. Climate change impacts on runoff, sediment, and nutrient loads in an agricultural watershed in the Lower Mississippi River Basin. *Appl. Eng. Agric.* **2017**, *33*, 379–392. [[CrossRef](#)]

**Publisher’s Note:** MDPI stays neutral with regard to jurisdictional claims in published maps and institutional affiliations.



© 2020 by the authors. Licensee MDPI, Basel, Switzerland. This article is an open access article distributed under the terms and conditions of the Creative Commons Attribution (CC BY) license (<http://creativecommons.org/licenses/by/4.0/>).